Available online at http://scik.org

Commun. Math. Biol. Neurosci. 2024, 2024:14

https://doi.org/10.28919/cmbn/8356

ISSN: 2052-2541

PARAMETERS ESTIMATION OF A MATHEMATICAL MODEL OF COVID-19 TRANSMISSION IN EAST JAVA PROVINCE USING THE DEEP LEARNING METHOD

BAYU SETIAWAN, ANITA TRISKA*, NURSANTI ANGGRIANI

Department of Mathematics, Universitas Padjadjaran, Sumedang 45363, Indonesia

Abstract: Coronavirus disease (Covid-19) is a respiratory disease caused by the Severe Acute Respiratory Syndrome Coronavirus 2 (SARS-CoV-2) virus which has spread throughout the world and becomes a pandemic in 2020. The spread of Covid-19 in Indonesia is fluctuating depend on people's habits and government policies which results in the time-dependent parameters. In this study, the spread of Covid-19 is analyzed by using a mathematical model through a system of Ordinary Differential Equations (ODE) which its parameters change respect to time. This study focuses on the time-dependent parameters which are estimated using the Deep Learning method based on the Covid-19 data from East Java Province, Indonesia. Furthermore, numerical simulation results of the model with time-dependent parameters are compared to numerical simulation results which use constant parameters. It is found that the simulation results of the model with time-dependent parameters are closer to the data with a Mean Absolute Percentage Error (MAPE) value is 3.68%, while the model with constant parameters had a MAPE value as 24.5%.

Keywords: covid-19; mathematical model; deep learning; dynamics system.

2020 AMS Subject Classification: 92D25, 92D30, 68T07.

*Corresponding author

E-mail address: a.triska@unpad.ac.id

Received November 21, 2023

1. INTRODUCTION

In last two years, the world experiences a health, social, and economic crisis caused by the pandemic of Coronavirus disease 2019 (Covid-19) which also occurs in Indonesia. This disease is caused by the Severe Acute Respiratory Syndrome Coronavirus 2 (SARS-CoV-2) which has spread throughout the world and become an outbreak. SARS-Cov2 has a spherical or elliptical shape and is about 60-140 nm in diameter [1]. Covid-19 is a very dangerous disease because it can cause death by its rapid spread process regardless of gender or age. The SARS-CoV-2 virus spreads through respiratory droplets produced by sneezing, coughing, and normal breathing. Symptoms of Covid-19 appear after an incubation period of approximately 5.2 days. The period from the onset of Covid-19 symptoms to death ranged from 6 to 41 days with 14 days in average [2]. The condition of infected individuals by Covid-19 can be divided into two categories, namely symptomatic infection and asymptomatic infection [3]. Since 15 March 2020, there have been 4.22 million confirmed cases and 145,000 deaths due to Covid-19 in Indonesia [4,5]. Several efforts have been made by the Indonesian government to deal with Covid-19, such as by enforcing health protocols, limiting population mobility by working from home, and holding a free vaccination program [6].

The development of mathematical knowledge also plays an important role in anticipating the spread of Covid-19. Until now, many studies have been done from mathematics point of view related to Covid-19 to ensure human survival. Many mathematical models illustrate the spread of Covid-19 by using a system of differential equations [8] through the compartment approach which is known as epidemic model. From those models, mathematical models have been developed to predict the Covid-19 epidemic [8-11]. Mathematical models of the spread of infectious diseases can be used to evaluate the process of epidemic transmission, but the values of parameters used in the model are mostly based on assumptions. The unknown parameters need to be estimated with the model fitting which makes the model more uncertain [12]. For a long duration of the spread of Covid-19, the change of the parameters value in model may occur which is caused by various reasons. For instance, the government policies in a country will affect the Covid-19 transmission

which also affect the parameters value. It is a challenge to construct a model with a single parameter to fit the real situation well [13]. In addition, previous researchers have also predicted the spread of Covid-19 by an epidemic model through the machine learning method that able to estimate the certain parameter which result in a simulation close to the data [14-18]. However, using the machine learning method only to predict Covid-19 cases cannot capture the patterns of the change of infectious disease transmission time by time [19]. To overcome the long duration of the spread of Covid-19 and the shortcomings of machine learning methods in prediction, Chen et. al. [20] proposed an SIR epidemic model which parameters change with time. Now, the model is known as the time-dependent SIR model. This method aims to make the model more adaptive since in reality the spread of Covid-19 is very volatile [20]. In the Covid-19 epidemic model with time-dependent parameters, its parameters can be estimated by using the Deep Learning method [21-24]. Parameters fluctuation in the model with time-dependent parameters are also influenced by government policies and people's habits [25].

Since the Machine Learning method success to estimate the parameters of a simple epidemic model, then in this study we develop a Covid-19 transmission model with time-dependent parameters with more complex compartments to obtain a more realistic model. In the present study we consider the infected population, which is divided into two categories namely symptomatic and asymptomatic-infected, including the addition of exposed population. Moreover, the model is also equipped by vaccination population as a representation of one of the government’s efforts in deal with Covid-19 in Indonesia. After that, a series of numerical simulation of the model with time-dependent parameters is implemented and compared to the numerical results of model whose parameters are constant to show which one is better to describes the actual conditions of the spread of Covid-19 in East Java, Indonesia. Here, the constant parameters are estimated by using the Least-Square method, while the time-dependent parameters are estimated using the Deep Learning method.

This paper is organized as follows. In Section 2, the research methods are discussed briefly, such as the Gershgorin theorem which is used to analyze the stability of equilibrium points and the

Deep Learning method. The results of this study are presented in Section 3. First, we construct the Covid-19 transmission model, followed by determining the stability of the disease-free and endemic equilibrium points and basic reproduction number as well. Next, the estimations of constant and time-dependent parameters are carried out and performed the numerical simulation results. Finally, we present the brief remarks of this study in the last section.

2. MATERIALS AND METHODS

2.1. Differential Equation System

An Ordinary Differential Equation (ODE) is an equation that involves the derivative of one dependent variable and one independent variable, while the system of differential equations is a collection of two or more differential equations. Systematically, the system of differential equations can be written in the form

$$\dot{\mathbf{x}}(t) = \mathbf{f}(\mathbf{x}, t), \tag{1}$$

where

$$\dot{\mathbf{x}}(t) = \begin{pmatrix} \frac{dx_1}{dt} \\ \frac{dx_2}{dt} \\ \vdots \\ \frac{dx_n}{dt} \end{pmatrix}, \qquad \mathbf{f}(\mathbf{x}, t) = \begin{pmatrix} f_1(t, x_1, x_2, \dots, x_n) \\ f_2(t, x_1, x_2, \dots, x_n) \\ \vdots \\ f_n(t, x_1, x_2, \dots, x_n) \end{pmatrix}, \tag{2}$$

2.2. Time-dependent Epidemic Model

The model is based on the SIR model with its parameters being a function of time which can be represented by

$$\begin{aligned} \frac{dS(t)}{dt} &= -\frac{\beta(t)S(t)I(t)}{N}, \\ \frac{dI(t)}{dt} &= \frac{\beta(t)S(t)I(t)}{N} - \gamma(t)I(t), \\ \frac{dR(t)}{dt} &= \gamma(t)I(t). \end{aligned} \tag{3}$$

Then, System (3) can be transformed into a differential equation with discrete time

$$\begin{aligned} S(t+1) - S(t) &= -\frac{\beta(t)S(t)I(t)}{n}, \\ I(t+1) - I(t) &= \frac{\beta(t)S(t)I(t)}{n} - \gamma(t)I(t), \\ R(t+1) - R(t) &= \gamma(t)I(t). \end{aligned} \tag{4}$$

By solving System (4) with respect to the parameters to be estimated so that the parameter equations that depend on time are obtained as follows

$$\begin{aligned} \gamma(t) &= \frac{R(t+1) - R(t)}{I(t)}, \\ \beta(t) &= \frac{\big(I(t+1) - I(t)\big) + \big(R(t+1) - R(t)\big)}{I(t)}. \end{aligned} \tag{5}$$

System (5) can be used to obtain parameters at any time needed [20].

2.3. Equilibrium Point

A continuous dynamic system is said to have an equilibrium point if the system of differential equations $\dot{\mathbf{x}} = \mathbf{f}(\mathbf{x})$ has a solution for $\mathbf{f}(\mathbf{x}) = 0$. The point x^* where $\mathbf{f}(x^*) = 0$ is satisfied is called the equilibrium point. In this state, the length of the tangent vector is zero and the system is said to be in equilibrium. In a homogeneous system, the trivial solution $\mathbf{x} = 0$ of $\mathbf{f}(\mathbf{x}) = 0$ is always an equilibrium state [27].

2.4. Basic Reproduction Number

The Basic Reproduction Number is the average number of second-infected individuals due to contracting the first-infected individual in a susceptible population [28]. First, determining the new infection vector and the displacement vector from the model that satisfies the

$$\dot{\mathbf{x}} = f_i(x) = \mathcal{F}_i(x) - \mathcal{V}_i(x), \qquad i = 1, \dots, n. \tag{6}$$

Next, convert the vector in Equation (6) into a matrix that satisfies

$$F = \left[\frac{\partial \mathcal{F}_i}{\partial x_j}(x_0^*)\right] \text{ and } V = \left[\frac{\partial \mathcal{V}_i}{\partial x_j}(x_0^*)\right], \qquad 1 \le i, j, \le m. \tag{7}$$

The basic reproduction number is determined through the next generation matrix by operating FV^{-1}. The largest eigenvalue of the next generation matrix is the basic reproduction number.

2.5. Gershgorin Theorem

Suppose there is a matrix $A = (a_{ij})$ then every eigenvalue of matrix A will satisfies

$$|\lambda - a_{ii}| \leq \sum_{j \neq i} |a_{ij}| \qquad i \in \{1,2,3, \dots, n\} \tag{8}$$

where λ is the eigenvalue of matrix A. Matrix $\lambda I - A$ is Strictly Diagonally Dominant Matrices $|\lambda - a_{ii}| > \sum_{j \neq i} |a_{ij}|$ for every i. if Equation (8) is not satisfied then $\lambda I - A$ is Strictly Diagonally Dominant Matrices. And if $\lambda I - A$ is Strictly Diagonally Dominant Matrices then the result λ is not an eigenvalue because the matrix $\lambda I - A$ nonsingular [29].

2.6. Stability Analysis Equilibrium Point using Gershgorin Discs

Let $A = (a_{ij})$ be a complex square matrix. Then each eigenvalue of A lies in one of the Gershgorin discs

$$D_i = \{z \in \mathbb{C} : |z - a_{ii}| \leq R_i\} \quad \vee \quad D_j = \{z \in \mathbb{C} : |z - a_{jj}| \leq R_j\} \tag{9}$$

where $R_i = \sum_{j=1, j \neq i}^{n} |a_{ij}|$ and $R_j = \sum_{i=1, i \neq j}^{n} |a_{ij}|$. The union of n Gershgorin discs is called the Gershgorin set.

$$D = \bigcup_{i=1}^{n} D_i \tag{10}$$

It can be observed that D is closed and finite in C, and all eigenvalues of A are elements of D. Let x^* be an equilibrium point of the system and the Jacobi Matrix of the system evaluated in x^* is

$$D\mathbf{f}(x^*) = \begin{pmatrix} J_{11} & J_{12} & \cdots & J_{1n} \\ J_{21} & J_{22} & \cdots & J_{2n} \\ \vdots & \vdots & \ddots & \vdots \\ J_{n1} & J_{n2} & \cdots & J_{nn} \end{pmatrix} \tag{11}$$

and

$$R_i = \sum_{j=1, j \neq i}^{n} |J_{ij}| \tag{12}$$

for $i = 1,2, \dots, n$. If $J_{ii} < 0$ and $R_i < |J_{ii}|$ then x^* is locally asymptotically stable. Since J_{ii} is the center point of the Gershgorin Disc is on the negative real axis of the complex plane and R_i

is the radius, so if $R_i < |J_{ii}|$ the disc is completely in the negative part of the complex plane and all the eigenvalues are negative [30].

3. MAIN RESULTS

3.1. Mathematical Model

Mathematical model in the present study is constructed through a compartment approach. Here, the population is divided into six subpopulations, namely susceptible, vaccinated, exposed, symptomatic, asymptomatic, and recovered population. The proposed model of the Covid-19 transmission in this study is equipped with the following assumptions.

A1. The population is assumed a closed population whose birth and death rates per time unit are considered constant.

A2. The population is homogeneous which means that each individual has the same chance of being infected.

A3. Vaccine is only given to the susceptible individuals.

A4. The vaccine efficacy is not permanent so that individuals who have been vaccinated can revert to being susceptible individuals after certain time [31].

A5. There is a latent period in the disease infection process, i.e., a condition in which an infected individual does not transmit the disease to other individuals.

Based on the above assumptions, the Covid-19 transmission can be described into a schematic diagram as follows

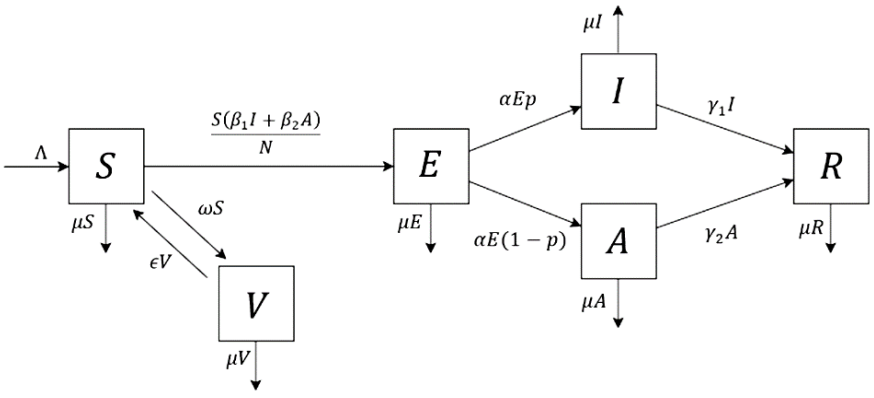

FIGURE 1. Schematic diagram of Covid-19 spread model.

Based on Figure 1, the Covid-19 transmission model can be written in the form of an equation system as follows:

$$\begin{aligned}
\frac{dS}{dt} &= \Lambda + \epsilon V - \frac{S(\beta_1 I + \beta_2 A)}{N} - (\omega + \mu)S, \\
\frac{dV}{dt} &= \omega S - (\mu + \epsilon)V, \\
\frac{dE}{dt} &= \frac{S(\beta_1 I + \beta_2 A)}{N} - (\alpha + \mu)E, \\
\frac{dI}{dt} &= \alpha E p - \gamma_1 I - \mu I, \\
\frac{dA}{dt} &= \alpha E(1-p) - \gamma_2 A - \mu A, \\
\frac{dR}{dt} &= \gamma_1 I + \gamma_2 A - \mu R,
\end{aligned} \tag{13}$$

with

S : Susceptible population,

V : Vaccinated population,

E : Expossed population,

I : Symptomatic population,

A : Asymptomatic population,

R : Recovered population,

Λ : Recruitment rate,

μ : Natural death rate,

ω : Vaccination rate,

ϵ : The rate of decline in immunity,

β_1 : Infection rate due to contact with symptomatic population,

β_2 : Infection rate due to contact with asymptomatic population,

α : Rate of the exposed individual becomes infected,

p : Rate of an infected individual being symptomatic,

γ_1 : Recovery rate of the symptomatic population,

γ_2 : Recovery rate of the asymptomatic population.

In order to simplify System (13), normalization is performed by dividing each subpopulation by the total population. First, introducing

$$\bar{S} = \frac{S}{N}, \bar{V} = \frac{V}{N}, \bar{E} = \frac{E}{N}, \bar{I} = \frac{I}{N}, \bar{A} = \frac{A}{N}, \text{ and } \bar{R} = \frac{R}{N}, \tag{14}$$

Substituting Equations in (14) into System (13) and removing the bar mark in each compartment notation for writing simplification, then the normalized model is obtained as follows

$$\begin{aligned}
\frac{dS}{dt} &= \Lambda + \epsilon V - S(\beta_1 I + \beta_2 A) - (\omega + \mu)S, \\
\frac{dV}{dt} &= \omega S - (\mu + \epsilon)V, \\
\frac{dE}{dt} &= S(\beta_1 I + \beta_2 A) - (\alpha + \mu)E, \\
\frac{dI}{dt} &= \alpha E p - \gamma_1 I - \mu I, \\
\frac{dA}{dt} &= \alpha E(1 - p) - \gamma_2 A - \mu A, \\
\frac{dR}{dt} &= \gamma_1 I + \gamma_2 A - \mu R,
\end{aligned} \tag{15}$$

with $S + V + E + I + A + R = 1$ and $\Lambda = \mu$.

3.2. Equilibrium Points and Basic Reproduction Number

In this section, equilibrium points and basic reproduction number of System (14) are performed. According to Section 2.3, System (15) has two equilibrium points, they are disease-free and endemic equilibrium points. In practice, one may obtain equilibrium points simultaneously. But in this paper, we display the basic reproduction number after the disease-free equilibrium points. As a result, the endemic equilibrium can be denoted in terms of basic reproduction number to provide simpler writing and analyzing.

3.2.1 Disease-free Equilibrium Point

The disease-free equilibrium point represents the situation of the population which is free from Covid-19. It means that infected individuals will vanish by themselves in the population and stays to be in a disease-free situation all the time. Here, the disease-free equilibrium is denoted by E_0, namely

$$E_0 = \left(S = \frac{(\mu+\epsilon)\Lambda}{\mu(\epsilon+\mu+\omega)}, V = \frac{\Lambda\omega}{\mu(\epsilon+\mu+\omega)}, E = 0, I = 0, A = 0, R = 0 \right).$$

From the biological point of view, the disease-free equilibrium point E_0 always exists since all populations are non-negative as the result of positivity of all parameters.

3.2.2 Basic Reproduction Number

The basic reproduction number of System (15) can be obtained by using the Next Generation Matrix method in Section 2.4. The compartments that affect the spread of Covid-19 are E, I, and A populations so that the Next Generation Matrix of System (15) is obtained as follows

$$FV^{-1} = \begin{bmatrix} a_{11} & \frac{(\mu+\epsilon)\Lambda\beta_1}{\mu(\mu+\epsilon+\omega)(\gamma_1+\mu)} & \frac{(\mu+\epsilon)\Lambda\beta_2}{\mu(\mu+\epsilon+\omega)(\gamma_2+\mu)} \\ 0 & 0 & 0 \\ 0 & 0 & 0 \end{bmatrix}, \tag{16}$$

with

$$a_{11} = \frac{(\mu+\epsilon)\Lambda\alpha\left(p\beta_1(\mu+\gamma_2) + \beta_2(1-p)(\mu+\gamma_1)\right)}{\mu(\mu+\epsilon+\omega)(\alpha+\mu)(\gamma_1+\mu)(\gamma_2+\mu)}. \tag{17}$$

Therefore, the spectral radius of Matrix (16) which is the basic reproduction number is

$$R_0 = \frac{(\mu+\epsilon)\Lambda\alpha\left(p\beta_1(\mu+\gamma_2) + \beta_2(1-p)(\mu+\gamma_1)\right)}{\mu(\mu+\epsilon+\omega)(\alpha+\mu)(\gamma_1+\mu)(\gamma_2+\mu)}. \tag{18}$$

3.2.3. Endemic Equilibrium Point

The endemic point represents a situation where Covid-19 spreads within the population and will always occur in the population over time. The endemic equilibrium point of System (15) is represented in term of R_0 in Equation (18) to get the following results

$$E_1 = (S^*, V^*, E^*, I^*, A^*, R^*), \tag{19}$$

with

$$\begin{aligned} S^* &= \frac{(\mu+\epsilon)\Lambda}{\mu(\mu+\epsilon+\omega)R_0}, & V^* &= \frac{\omega\Lambda}{\mu(\mu+\epsilon+\omega)R_0}, \\ E^* &= \frac{\Lambda(R_0-1)}{(\alpha+\mu)R_0}, & I^* &= \frac{\alpha\Lambda(R_0-1)\mathrm{p}}{(\alpha+\mu)(\mu+\gamma_1)R_0}, \\ A^* &= \frac{\alpha\Lambda(R_0-1)(1-p)}{(\alpha+\mu)(\mu+\gamma_2)R_0}, & R^* &= \frac{(\mu p\gamma_1 + \gamma_1\gamma_2 + \mu\gamma_2(1-p))\alpha\Lambda(R_0-1)}{(\mu+\gamma_2)(\alpha+\mu)(\mu+\gamma_1)\mu R_0} \end{aligned} \tag{20}$$

The representation of endemic equilibrium point in term of R_0 makes it easy to analyze. Since all

parameters involved in System (15) are non-negative and $0 < p < 1$ then the existence condition of E_1 is $R_0 > 1$.

3.3. Equilibrium Point Stability Analysis

3.3.1. Disease-free equilibrium stability

The stability of equilibrium points in this study is analyzed by using the eigenvalues approach. The mathematical calculation to determine the stability of equilibrium points of System (15) is complex enough. Thus, for simplification it is assumed that the infection rate by asymptomatic and symptomatic individuals are the same ($\beta_1 = \beta_2$). The eigenvalues which correspond to each equilibrium point are detected by Gershgorin disc approach according to Section 2.5.

First, determining the Jacobian matrix of System (15) than we obtain

$$J = \begin{pmatrix} -A\beta_2 - I\beta_1 - \mu - \omega & \epsilon & 0 & -S\beta_1 & -S\beta_2 & 0 \\ \omega & -\epsilon - \mu & 0 & 0 & 0 & 0 \\ A\beta_2 + I\beta_1 & 0 & -\alpha - \mu & S\beta_1 & S\beta_2 & 0 \\ 0 & 0 & \alpha p & -\mu - \gamma_1 & 0 & 0 \\ 0 & 0 & \alpha(1-p) & 0 & -\gamma_2 - \mu & 0 \\ 0 & 0 & 0 & \gamma_1 & \gamma_2 & -\mu \end{pmatrix}.$$

Next, evaluating the Jacobian matrix J at E_0 so that the following result is yielded

$$J(E_0) = \begin{pmatrix} -\mu - \omega & \epsilon & 0 & -\frac{(\mu+\epsilon)\Lambda}{\mu(\epsilon+\mu+\omega)}\beta & -\frac{(\mu+\epsilon)\Lambda}{\mu(\epsilon+\mu+\omega)}\beta & 0 \\ \omega & -\epsilon - \mu & 0 & 0 & 0 & 0 \\ 0 & 0 & -\alpha - \mu & \frac{(\mu+\epsilon)\Lambda}{\mu(\epsilon+\mu+\omega)}\beta_1 & \frac{(\mu+\epsilon)\Lambda}{\mu(\epsilon+\mu+\omega)}\beta_2 & 0 \\ 0 & 0 & \alpha p & -\mu - \gamma_1 & 0 & 0 \\ 0 & 0 & \alpha(1-p) & 0 & -\gamma_2 - \mu & 0 \\ 0 & 0 & 0 & \gamma_1 & \gamma_2 & -\mu \end{pmatrix}.$$

It is clear that all elements of the diagonal of matrix $J(E_0)$ are negative so that based on the Gershgorin theory the center point of the Gershgorin disc is in the negative plane. To ensure all discs are in the negative plane so that all eigenvalues are negative as well, then the radius of the whole discs must be $R_i < J_{ii}$ with $i = 1,2, \dots ,6$.

As the consequences, the disease-free equilibrium point E_0 is local asymtotically stable if all of the eigenvalues of the correspond Jacobian matrix $(J(E_0))$ satisfy at least one of the following Gershgorin discs, i.e.

$$\epsilon + \frac{2\beta(\mu+\epsilon)\Lambda}{\mu(\epsilon+\mu+\omega)} < \mu + \omega, \qquad \omega < \mu + \epsilon,$$
$$\frac{2\beta(\mu+\epsilon)\Lambda}{\mu(\epsilon+\mu+\omega)} < \mu + \alpha, \qquad \gamma_1 + \gamma_2 < \mu,$$
$$\alpha p < \mu + \gamma_1, \qquad \alpha(1-p) < (\mu + \gamma_2).$$

These Gershgorin discs condition or some of them can be simplified or represented in term of R_0 as follows

$$R_0 < 1, \qquad \beta\Lambda < 2, \quad \gamma_1 + \gamma_2 < \mu. \tag{21}$$

The second inequality in conditions (21) is always fulfilled so that it is not an asymptotically stable condition since the recruitment rate Λ is biologically less than 1, and the parameter $\beta \in (0,1)$. Meanwhile, the third inequality is biologically impossible to occur because μ is the rate of natural death is not the death rate from disease is not greater than the sum of the recovery rates from symptomatic (γ_1) and asymptomatic (γ_2) infections. Thus, the stability requirement for a disease-free point is $R_0 < 1$.

In other words, the disease will disappear from the population if at least one or more of the Gershgorin discs condition in (21) are satisfied. For the first inequality in (21), the disease-free equilibrium will be stable if this condition is met because if the basic reproduction number is less than 1 or each infected individual transmits the disease to less than one new individual, the number of infections in a population will decrease. For the second inequality, it means that it will be stable if β or the rate of infection, both asymptomatic and symptomatic infections multiplied by the rate of recruitment into the ecosystem is less than 2, meaning that the value of the rate of infection is small so that fewer individuals are infected. For the third inequality, the total value of the recovery rate is smaller than the value of the death parameter. In the case of $R_0 < 1$ the value of the recovery rate is relatively large so that a greater value of the death rate will remove the population from the infected and recovered compartments while the susceptible population will still exist because the recruitment rate is the same as the death rate.

The disease-free point is asymptotically stable if it satisfies at least one Gershgorin Disc in System (21). The second inequality in System (21) is always satisfied so that it is not an asymptotically stable condition because the recruitment rate (Λ) is biologically impossible to

hold a value greater than 1, and the infection rate parameter (β) is not possible to be greater than 2. At the same time, the third inequality is not biologically possible because it is the pure death rate (μ), not the death rate due to disease, and not greater than the sum of the cure rates for symptomatic (γ_1) and asymptomatic (γ_2). Accordingly, the stability required for the disease-free point is $R_0 < 1$.

3.5.2. Endemic equilibrium stability

The stability analysis of endemic equilibrium point E_1 is carried out by doing the same prosedur as the stability analysis of E_0. Substituting E_1 to the Jacobian matrix J yield

$$J(E_1) = \begin{pmatrix} a_{11} & \epsilon & 0 & -\frac{(\mu+\epsilon)\Lambda}{\mu(\mu+\epsilon+\omega)R_0}\beta_1 & -\frac{(\mu+\epsilon)\Lambda}{\mu(\mu+\epsilon+\omega)R_0}\beta_2 & 0 \\ \omega & -\epsilon-\mu & 0 & 0 & 0 & 0 \\ a_{31} & 0 & -\alpha-\mu & \frac{(\mu+\epsilon)\Lambda}{\mu(\mu+\epsilon+\omega)R_0}\beta_1 & \frac{(\mu+\epsilon)\Lambda}{\mu(\mu+\epsilon+\omega)R_0}\beta_2 & 0 \\ 0 & 0 & \alpha p & -\mu-\gamma_1 & 0 & 0 \\ 0 & 0 & \alpha(1-p) & 0 & -\gamma_2-\mu & 0 \\ 0 & 0 & 0 & \gamma_1 & \gamma_2 & -\mu \end{pmatrix}$$

with

$$a_{11} = -\frac{\alpha\Lambda(R_0-1)(1-p)}{(\alpha+\mu)(\mu+\gamma_2)R_0}\beta_2 - \frac{\alpha\Lambda(R_0-1)\mathrm{p}}{(\alpha+\mu)(\mu+\gamma_1)R_0}\beta_1 - \mu - \omega,$$

$$a_{31} = \frac{\alpha\Lambda(R_0-1)(1-p)}{(\alpha+\mu)(\mu+\gamma_2)R_0}\beta_2 + \frac{\alpha\Lambda(R_0-1)\mathrm{p}}{(\alpha+\mu)(\mu+\gamma_1)R_0}\beta_1.$$

It is clear that a_{11} is negative so that all elements of the diagonal of matrix $J(E_1)$ are negative result in the center point of the Gershgorin disc is in the negative plane. The endemic equilibrium point is asymptotically stable if $R_0 > 1$ and hold at least one of the following Gershgorin disc,

$$\epsilon + \frac{(\beta_1+\beta_2)(\mu+\epsilon)\Lambda}{\mu(\epsilon+\mu+\omega)R_0} < \frac{\alpha\Lambda(R_0-1)(1-p)}{(\alpha+\mu)(\mu+\gamma_2)R_0}\beta_2 + \frac{\alpha\Lambda(R_0-1)\mathrm{p}}{(\alpha+\mu)(\mu+\gamma_1)R_0}\beta_1 + \mu + \omega,$$

$$\omega < \mu + \epsilon,$$

$$\frac{\alpha\Lambda(R_0-1)(1-p)}{(\alpha+\mu)(\mu+\gamma_2)R_0}\beta_2 + \frac{\alpha\Lambda(R_0-1)\mathrm{p}}{(\alpha+\mu)(\mu+\gamma_1)R_0}\beta_1 + \frac{(\beta_1+\beta_2)(\mu+\epsilon)\Lambda}{\mu(\epsilon+\mu+\omega)R_0} < \mu + \alpha,$$

$$\gamma_1 + \gamma_2 < \mu, \qquad \alpha p < \mu + \gamma_1, \qquad \alpha(1-p) < (\mu + \gamma_2),$$

These Gershgorin discs condition or some of them can be simplified or represented in term of R_0

as follows

$$\Lambda\beta < 2R_0 \quad \text{and} \quad \gamma_1 + \gamma_2 < \mu, \tag{22}$$

with $R_0 > 1$.

The disease will exist in the population or be endemic provided that $R_0 > 1$ must be met before then being determined with at least one of the Gershgorin discs in System (22) being met. This means that the disease is transmitted from an infected individual to more than one susceptible individual so that the infected population will increase. Then the first inequality in System (22) the value of the recruitment rate multiplied by the infection rate is less than twice the basic reproduction number where $R_0 > 1$ so that the right side will increase the β value limit or the infection rate will be greater when compared to the gershorin disc system (21) a large recruitment rate value will increase the infected population. Then the second inequality in system (22) where previously the value of $R_0 > 1$ must be fulfilled first so that the recovery value will be relatively small, causing individuals in the infected compartment not to move much to the recovered compartment.

However, the endemic point is asymptotically stable if $R_0 > 1$ and satisfies at least one Gershgorin disk in Equation (22). The first inequality in System (22) is always fulfilled because it has a mandatory condition of $R_0 > 1,$ and biologically, it is not possible to have a recruitment rate (Λ) and an infection rate (β) that is greater than 2. Moreover, the second inequality in System (22) is biologically impossible to occur as stated in the previous explanation. Therefore, the stability condition for the endemic point is $R_0 > 1$.

3.4. Parameters Estimation

In this study, estimation of several parameters is carried out in two ways, i.e., constant and time-dependen parameters. The time-dependent estimation parameters is considered to capture the fluctuation of parameters value due to government policies and people's habits during the Covid-19 pandemic. Here, parameter $\alpha, \beta_1, \beta_2, \gamma_1$ and γ_2 are choosen to be estimated since these parameters are one of the core parameters of the model and related to running policies.

3.4.1. Constant Parameters Estimation

Constant parameters estimation is carried out by using the Least-Square method. Here, the data of Covid-19 cases in East Java Province, Indonesia, is collected from February 18 until April 8, 2022. Those data are used to be the initial values of each population which is displayed in Table 1 and followed by other parameters that are not estimated.

TABLE 1. Variables and parameters values.

Parameters	**Value**	**Reference**
S	0.424455	[32]
V	0.563233	[32]
E	0.001051	[32]
I	0.000409	[32]
A	0.000367	[32]
R	0.010486	[32]
Λ	3.8602×10^{-5}	[33]
μ	3.8602×10^{-5}	[33]
p	0.45	Assumed
ω	0.026	Assumed
ϵ	0.015	Assumed

Constant parameters estimation is performed in two cases, namely $\beta_1 \neq \beta_2$ and $\beta_1 = \beta_2$. In the case of $\beta_1 \neq \beta_2$, the estimated parameters values are $\alpha = 0.1529$, $\beta_1 = 0.6619$, $\beta_2 = 2.444e^{-8}$, $\gamma_1 = 0.2607$, and $\gamma_2 = 0.2077$. Meanwhile, in the case of $\beta_1 = \beta_2$, the estimated parameter values obtained are $\alpha = 0{,}1563$, $\beta = 0{,}2851$, $\gamma_1 = 0{,}2162$, and $\gamma_2 = 0{,}2563$. Further, these results are analyzed in Section 3.5.

3.4.2. Time-dependent Parameter Estimation

Next, the time-dependent estimated parameters are performed by transforming System (15) into a differential equation with discrete time according to Section 2.2. Under this circumstance, the time-dependent estimated parameter can be done if it can be denoted explicitly from its original equation and not contained other estimated parameters. As a consequence, the time-dependent estimated parameters are only conducted in one case, namely $\beta_1 = \beta_2$, so that β_1 does not depends on β_2 and vice versa. Thus, the number of time-dependent parameters that can be estimated in System (15) are three parameters. Here, we decide to choose parameters $\beta_1 = \beta_2 = \beta, \gamma_1,$ and γ_2. By doing the same technique as in [20], we obtain the estimated parameter function

as follows

$$\begin{aligned}\beta(t) &= \frac{E(t+1) - E(t) + (\alpha+\mu)E(t)}{S(t)\big(I(t)+A(t)\big)},\\ \gamma_1(t) &= \frac{\alpha E(t)p - I(t+1) + I(t) - \mu I(t)}{I(t)},\\ \gamma_2(t) &= \frac{\alpha E(t)(1-p) - A(t+1) + A(t) - \mu A(t)}{A(t)}.\end{aligned} \tag{23}$$

Next, System (15) is transformed into a discrete mode as follows

$$\begin{aligned}S(t+1) &= S(t) + \Lambda + \epsilon(t)V(t) - S(t)\beta(t)\big(I(t)+A(t)\big) - (\omega+\mu)S(t),\\ V(t+1) &= V(t) + \omega S(t) - \mu V(t) - \epsilon(t)V(t),\\ E(t+1) &= E(t) + S(t)\beta(t)\big(I(t)+A(t)\big) - (\alpha+\mu)E(t),\\ I(t+1) &= I(t) + \alpha E(t)p - \gamma_1(t)I(t) - \mu I(t),\\ A(t+1) &= A(t) + \alpha E(t)(1-p) - \gamma_2(t)A(t) - \mu A(t),\\ R(t+1) &= R(t) + \gamma_1(t)I(t) + \gamma_2(t)A(t) - \mu R(t).\end{aligned} \tag{24}$$

There are several steps to obtain time-dependent parameters by using the Deep Learning method. First, dividing the data into two categories, i.e., the training and testing data with composition 70% and 30% of the data, respectively. The training data is used to train the Deep Learning model, while the testing data is used to compare the output of the Deep Learning estimation. The daily data representing the number of individuals each compartment is proceeded into Equations (23) to obtain time-dependent parameters value. After that, the time-dependent parameters value is smoothed so that the following results are obtained and displayed in Figure 2.

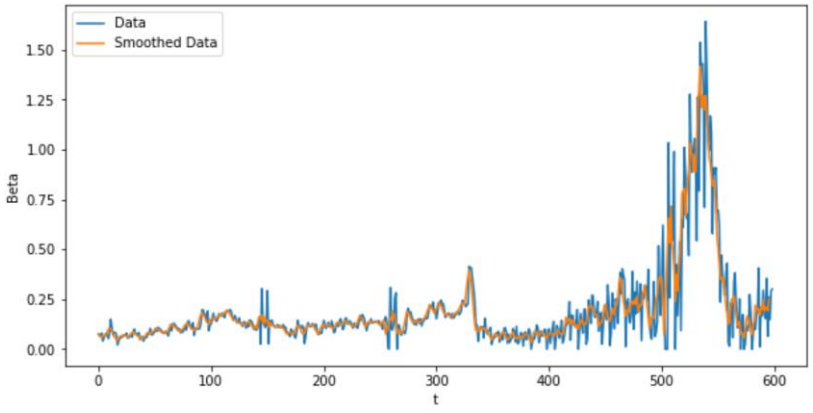

(a)

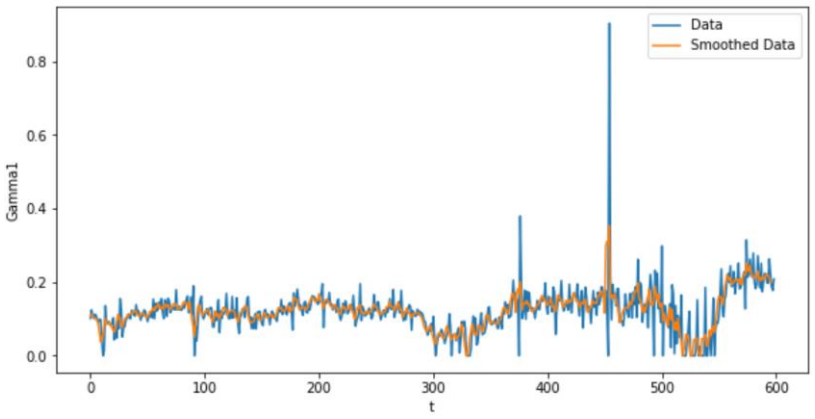

(b)

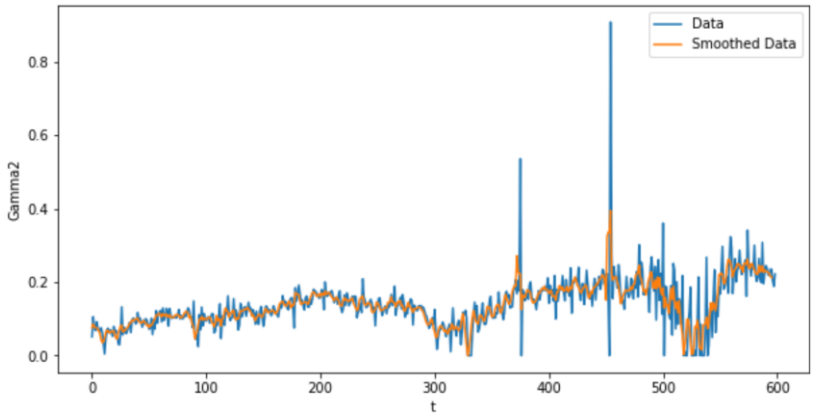

(c)

FIGURE 2. The results of data smoothing.

The data after smoothing as shown in Figure 2 of the orange line is then processed to become input data from the Deep Learning model. Data smoothing aims to eliminate outlier values that can interfere with the estimation results from Deep Learning. In addition, data smoothing also improves the performance of the Deep Learning model to be faster and more accurate [19]. Subsequently, creating a Long Short-term Memory (LSTM) model with three layers which each batch size is 16, 32, and 16. Next, setting each sigmoid recurrent activation function. Finally, using Adam's Optimizer for hyperparameter optimization on Deep Learning model and performing 500 epochs. The estimation results of the three parameters, $\beta, \gamma_1,$ and γ_2, are plotted in Figure 3.

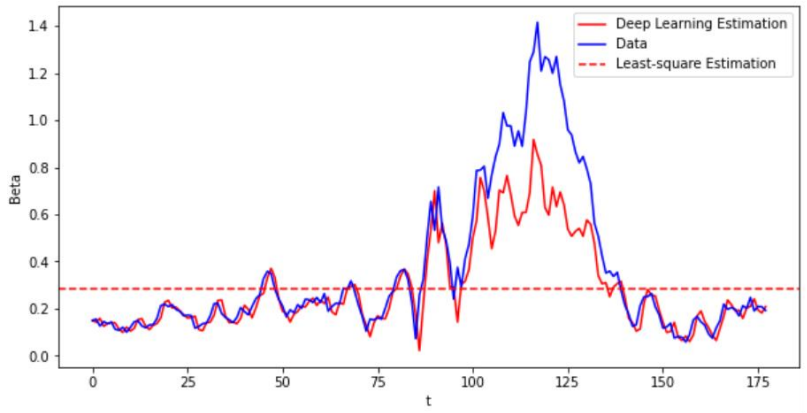

(a)

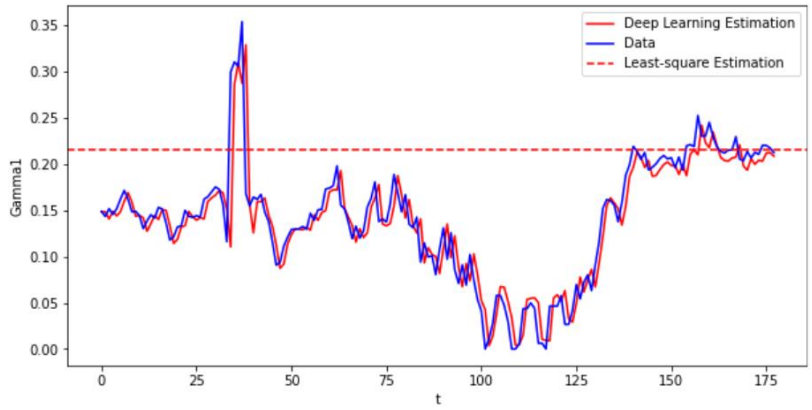

(b)

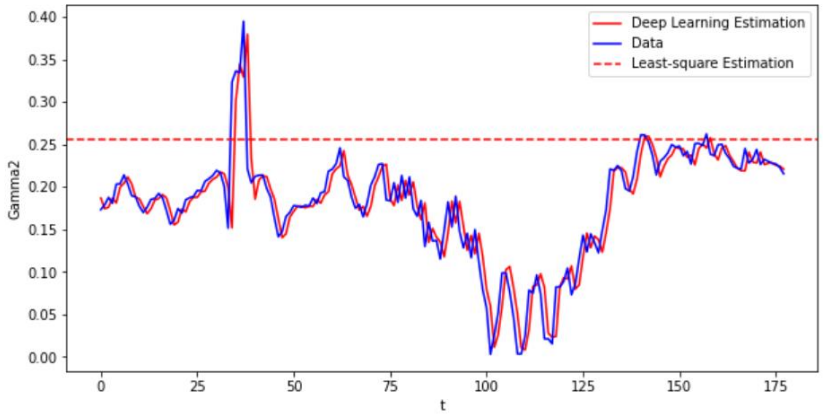

(c)

FIGURE 3. The estimation results of the time-dependent parameter.

It can be observed from Figure 3 that the Deep Learning method is able to produce the parameters values (red line) which is close to parameter values that is obtained from the data (blue

line). These results also show that the time-dependent parameters are much better at capturing the fluctuating parameter compared to the constant parameter. In Figure 3(a), during interval $t = 100$ to $t = 130$ there is a quite difference between the estimation results and the data. It is a consequence of the taken training data at the previous time is not experienced a very large increase of parameter value. However, it could still detect the increasing of parameter value. Meanwhile, the recovery rates γ_1 and γ_2 which can be seen in Figures 3(b) and 3(c) are able to be estimated by using the Deep Learning method, whereas constant parameter values estimated using the Least Square method can only approach the data at certain times.

3.5. Numerical Simulation

In this section, the numerical simulation of System (15) is performed with the parameter values that have been estimated, i.e., the constant parameters and time-dependent parameters. The initial values and other parameters use the values in Table 1. Numerical simulation results are seen in Figure 4.

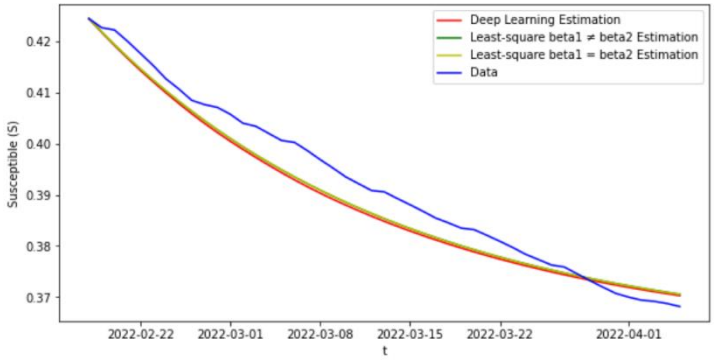

(a)

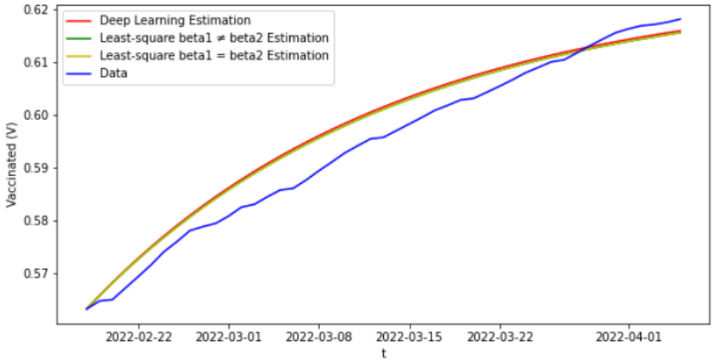

(b)

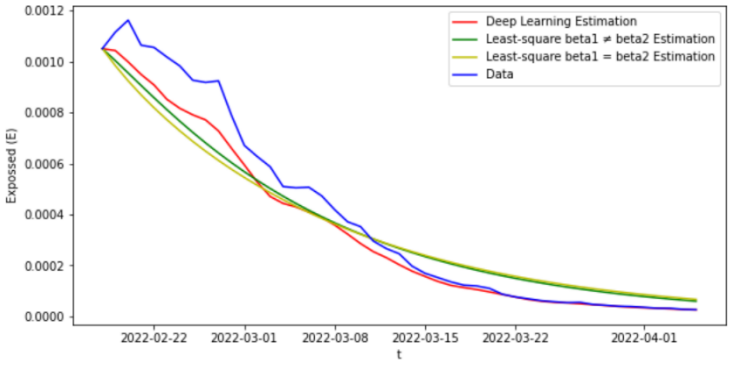

(c)

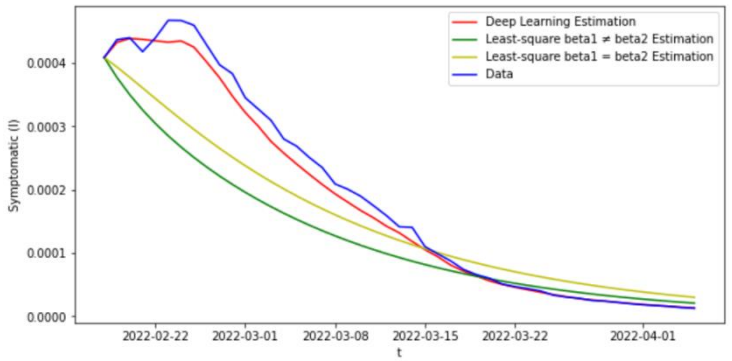

(d)

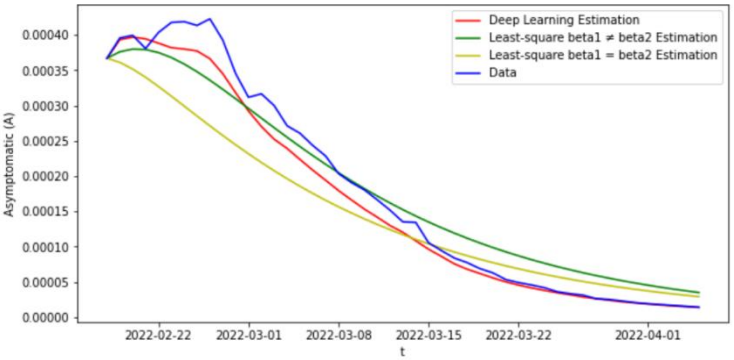

(e)

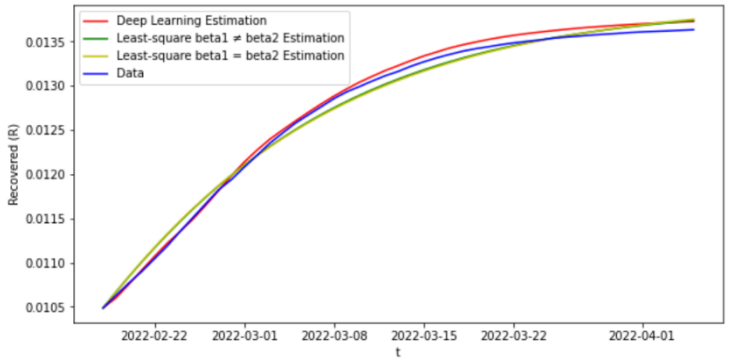

(f)

FIGURE 4. Numerical simulation results of each compartment.

The numerical simulation results of each compartment are displayed from the estimated parameters. (a) is the susceptible compartment, (b) is the vaccine compartment, (c) is the exposed compartment, (d) is the symptomatic compartment, (e) is the asymptomatic compartment, and (f) is the recovered compartment. The red line is a simulation of the model with parameters that change with time estimated using the Deep Learning method, while the green and yellow lines are numerical simulations of the model with constant parameters, and the blue line represents the data. Figure 4 shows the dynamics of each population which is produced by using parameter values yielded form the Deep Learning methods (red curve) and the Least Square method with two cases, namely $\beta_1 \neq \beta_2$ and $\beta_1 = \beta_2$ (green and yellow curve, respectively), where the blue line is the data. Based on Figure 4, it is can be observed that the overall dynamics results using the Deep Learning method are more accurate in approaching the data than the Least-square results with both cases, $\beta_1 = \beta_2$ and $\beta_1 = \beta_2$. In Figures 4(a), 4(b), and 4(f) there is not much difference between the various estimation results in the Susceptible, Vaccinated and Recovered compartments, but pay attention to Figures 4(c), 4(d), 4(e) which are the Exposed, Asymptomatic Infected and Symptomatic Infected compartments the data values are also smaller compared to the previous compartment. It is enough to see that the Deep Learning estimation results are more accurate in approaching the data then the pattern is also more appropriate where there is an increase first before finally decreasing. As has been done before, it is not only the pattern of changing parameters that can be followed by the Deep Learning method, but also the pattern of changing the population automatically follows like the data.

4. DISCUSSION

The MAPE is obtained by comparing data and the results of each estimation method. The MAPE calculation results for each method are as follows.

TABLE 2. MAPE of the estimation results from the constant and time-dependent parameters.

Compartments	**MAPE (%)**		
	Constant Parameter ($\beta_2 \neq \beta_2$)	Constant Parameter ($\beta_2 = \beta_2$)	Time-dependent Parameter
S	0.84589	0.84194	0.94499
V	0.58571	0.58690	0.62044
E	53.24760	61.12237	6.55554
I	33.47746	45.57388	5.78422
A	48.10107	38.48291	6.79970
R	0.53130	0.58038	1.40085
Average	**22.79817**	**24.53139**	**3.68429**

The smaller the MAPE, the better the accuracy of the method that has been done. Based on Table 2, it is observed that the model with Time-dependent parameters has the best accuracy with a MAPE value of 3.68%, followed by a model with constant parameters for $\beta_1 \neq \beta_2$ with a MAPE value of 22.79% and finally a model with constant parameters for $\beta_1 = \beta_2$ with a MAPE value of 24.53%. Thus, the use of time-dependent parameters can produce a very good model with significant accuracy. Besides that, the complexity of the model also produces a better model in terms of accuracy.

Constant and time-dependent parameters that have been estimated produce numerical simulations that are in accordance with the data. Based on Figure 3, estimation using Deep Learning is more accurate in compartments $E, I,$ and A because it is closer to the data value. A comparison can also be made based on the MAPE value. In the constant parameter estimation, the MAPE values are 22.79% and 24.53% in the case of $\beta_1 \neq \beta_2$ and $\beta_1 = \beta_2$, respectively. Whereas the parameters depend on the estimated time resulting in numerical simulations that correspond to the data with a MAPE value of 3.68%.

5. CONCLUSIONS

Analytically, the disease-free equilibrium points of the Covid-19 spread model are local asymptotically stable if $R_0 < 1$, while the endemic point is local asymptotically stable if $R_0 > 1$. The constant parameter estimation of the proposed model is carried out in the case of $\beta_1 \neq \beta_2$

and $\beta_1 = \beta_2$. From the estimated parameters, numerical simulations that correspond to the data yield the MAPE values of 22.79% and 24.53% in the case of $\beta_1 \neq \beta_2$ and $\beta_1 = \beta_2$, respectively. The estimation of time-dependent parameters in the model is only carried out in the case of $\beta_1 = \beta_2$. From the estimated parameters, numerical simulations yield a MAPE value of 3.68%. In general, time-dependent parameter estimation can give better simulation results since it produces the smallest MAPE value.

ACKNOWLEDGEMENTS

We would like to thank Universitas Padjadjaran for funding the APC of this article.

CONFLICT OF INTERESTS

The authors declare that there is no conflict of interests.

REFERENCES

[1] J.F.W. Chan, K.H. Kok, Z. Zhu, et al. Genomic characterization of the 2019 novel human-pathogenic coronavirus isolated from a patient with atypical pneumonia after visiting Wuhan, Emerg. Microbes Infect. 9 (2020), 221-236. https://doi.org/10.1080/22221751.2020.1719902.

[2] H.A. Rothan, S.N. Byrareddy, The epidemiology and pathogenesis of coronavirus disease (COVID-19) outbreak, J. Autoimmun. 109 (2020), 102433. https://doi.org/10.1016/j.jaut.2020.102433.

[3] Z. Wu, J.M. McGoogan, Characteristics of and important lessons from the coronavirus disease 2019 (COVID-19) outbreak in China, JAMA. 323 (2020), 1239-1242. https://doi.org/10.1001/jama.2020.2648.

[4] J. Hasell, E. Mathieu, D. Beltekian, et al. A cross-country database of COVID-19 testing, Sci. Data. 7 (2020), 345. https://doi.org/10.1038/s41597-020-00688-8.

[5] E. Dong, H. Du, L. Gardner, An interactive web-based dashboard to track COVID-19 in real time, Lancet Infect. Dis. 20 (2020), 533-534. https://doi.org/10.1016/s1473-3099(20)30120-1.

[6] I.K.S.L.P. Perbawa, The Indonesian government's policies in dealing with COVID-19 based on international legal instruments, J. Ilmu Sos. Human. 10 (2021), 197-205. https://doi.org/10.23887/jish-undiksha.v10i1.33517.

[7] W.O. Kermack, A.G. McKendrick, A contribution to the mathematical theory of epidemics, Proc. R. Soc. Lond. A. 115 (1927), 700-721. https://doi.org/10.1098/rspa.1927.0118.

[8] P. Singh, A. Gupta, Generalized SIR (GSIR) epidemic model: An improved framework for the predictive monitoring of COVID-19 pandemic, ISA Transactions. 124 (2022), 31-40. https://doi.org/10.1016/j.isatra.2021.02.016.

[9] Y. Wang, P. Wang, S. Zhang, et al. Uncertainty modeling of a modified SEIR epidemic model for COVID-19, Biology. 11 (2022), 1157. https://doi.org/10.3390/biology11081157.

[10] Q. Lin, S. Zhao, D. Gao, et al. A conceptual model for the coronavirus disease 2019 (COVID-19) outbreak in Wuhan, China with individual reaction and governmental action, Int. J. Infect. Dis. 93 (2020) 211-216. https://doi.org/10.1016/j.ijid.2020.02.058.

[11] M. Rangasamy, C. Chesneau, C. Martin-Barreiro, et al. On a novel dynamics of SEIR epidemic models with a potential application to COVID-19, Symmetry. 14 (2022), 1436. https://doi.org/10.3390/sym14071436.

[12] I. Holmdahl, C. Buckee, Wrong but useful — What Covid-19 epidemiologic models can and cannot tell us, N. Engl. J. Med. 383 (2020), 303-305. https://doi.org/10.1056/nejmp2016822.

[13] J. Panovska-Griffiths, Can mathematical modelling solve the current Covid-19 crisis?, BMC Public Health. 20 (2020), 551. https://doi.org/10.1186/s12889-020-08671-z.

[14] A. Zeroual, F. Harrou, A. Dairi, Y. Sun, Deep learning methods for forecasting COVID-19 time-Series data: A Comparative study, Chaos Solitons Fractals. 140 (2020), 110121. https://doi.org/10.1016/j.chaos.2020.110121.

[15] J. Devaraj, R.M. Elavarasan, R. Pugazhendhi, et al. Forecasting of COVID-19 cases using deep learning models: Is it reliable and practically significant?, Results Phys. 21 (2021), 103817. https://doi.org/10.1016/j.rinp.2021.103817.

[16] S. Shastri, K. Singh, S. Kumar, et al. Time series forecasting of Covid-19 using deep learning models: India-USA comparative case study, Chaos Solitons Fractals. 140 (2020), 110227. https://doi.org/10.1016/j.chaos.2020.110227.

[17] A.S. Fokas, N. Dikaios, G.A. Kastis, Mathematical models and deep learning for predicting the number of individuals reported to be infected with SARS-CoV-2, J. R. Soc. Interface. 17 (2020), 20200494. https://doi.org/10.1098/rsif.2020.0494.

[18] K.N. Nabi, M.T. Tahmid, A. Rafi, et al. Forecasting COVID-19 cases: A comparative analysis between recurrent and convolutional neural networks, Results Phys. 24 (2021), 104137. https://doi.org/10.1016/j.rinp.2021.104137.

[19] Z. Liao, P. Lan, X. Fan, et al. SIRVD-DL: A COVID-19 deep learning prediction model based on time-dependent SIRVD, Computers Biol. Med. 138 (2021), 104868. https://doi.org/10.1016/j.compbiomed.2021.104868.

[20] Y.C. Chen, P.E. Lu, C.S. Chang, et al. A time-dependent SIR model for COVID-19 with undetectable infected persons, IEEE Trans. Netw. Sci. Eng. 7 (2020), 3279-3294. https://doi.org/10.1109/tnse.2020.3024723.

[21] H. Jo, H. Son, H.J. Hwang, et al. Analysis of COVID-19 spread in South Korea using the SIR model with time-dependent parameters and deep learning, preprint, 2020. https://doi.org/10.1101/2020.04.13.20063412.

[22] R. Vega, L. Flores, R. Greiner, SIMLR: Machine learning inside the SIR model for COVID-19 forecasting, Forecasting. 4 (2022), 72-94. https://doi.org/10.3390/forecast4010005.

[23] Z. Liao, P. Lan, Z. Liao, et al. TW-SIR: time-window based SIR for COVID-19 forecasts, Sci. Rep. 10 (2020), 22454. https://doi.org/10.1038/s41598-020-80007-8.

[24] Y. Li, L. Ge, Y. Zhou, et al. Toward the impact of non-pharmaceutical interventions and vaccination on the COVID-19 pandemic with time-dependent SEIR model, Front. Artif. Intell. 4 (2021), 648579. https://doi.org/10.3389/frai.2021.648579.

[25] L.F. Castillo Ossa, P. Chamoso, J. Arango-López, et al. A hybrid model for COVID-19 monitoring and prediction, Electronics. 10 (2021), 799. https://doi.org/10.3390/electronics10070799.

[26] J.K. Hale, H. Koçak, Dynamics and bifurcations, Springer, New York, 1991. https://doi.org/10.1007/978-1-4612-4426-4.

[27] G. Fischel, E. Gröller, Visualization of local stability of dynamical systems, Eurographics. (1995), 106-117. https://doi.org/10.1007/978-3-7091-9425-6_10.

[28] P. van den Driessche, J. Watmough, Reproduction numbers and sub-threshold endemic equilibria for compartmental models of disease transmission, Math. Biosci. 180 (2002), 29–48. https://doi.org/10.1016/s0025-5564(02)00108-6.

[29] S. Gershgorin, Über die abgrenzung der eigenwerte einer matrix, Izv. Akad. Nauk. USSR Otd. Fiz.-Mat. Nauk. 6 (1931), 749-754.

[30] D.A. Ortega Bejarano, E. Ibarguen-Mondragon, E.A. Gomez-Hernandez, A stability test for non linear systems of ordinary differential equations based on the Gershgorin circles, Contemp. Eng. Sci. 11 (2018), 4541-4548. https://doi.org/10.12988/ces.2018.89504.

[31] P.V. Juthani, A. Gupta, K.A. Borges, et al. Hospitalisation among vaccine breakthrough COVID-19 infections, Lancet Infect. Dis. 21 (2021), 1485-1486. https://doi.org/10.1016/s1473-3099(21)00558-2.

[32] The Government of East Java Province. East Java COVID-19 Dashboard, 2022. https://covid19dev.jatimprov.go.id/xweb/drax/persebaran (accessed on 04 July 2022).

[33] Badan Pusat Statistik, Parameter Hasil Proyeksi Penduduk di Jawa Timur. https://jatim.bps.go.id/statictable/2018/02/05/840/parameter-hasil-proyeksi-penduduk-di-jawa-timur-2010-2035.html (accessed on 04 Juli 2022).